CAUCHY – Jurnal Matematika Murni dan Aplikasi
Volume 10 (2) (2025), Pages 1054-1068
p-ISSN: 2086-0382; e-ISSN: 2477-3344

Model of Three Species Commensalism-Amensalism Symbiosis with Beddington-DeAngelis Functional Responses

Nada Shofiyya, Wuryansari Muharini Kusumawinahyu*, and Ummu Habibah

Department of Mathematics, Faculty of Mathematics and Natural Sciences, University of Brawijaya, Indonesia

Abstract

This study investigates the dynamical behavior of a three species ecological system involving unilateral interactions of commensalism and amensalism with Beddington–DeAngelis functional responses. The positivity, boundedness, existence, and uniqueness of the model solutions are established, and four equilibrium points are identified. Stability analysis shows that the neutral-only and the coexistence equilibrium points are locally asymptotically stable, whereas the other equilibria are always unstable. Numerical simulations are conducted to confirm the analytical findings. Ecologically, the results indicate that stability can be achieved only when all neutral species coexist, even though without the commensal–amensal species. The existence of the commensal-amensal species is influenced by its own population density.

Keywords: amensalism; Beddington-DeAngelis functional response; commensalism; dynamical systems; local stability.

1 Introduction

Species interactions in ecosystems encompass various forms such as predation, competition, and symbiosis, which generally exert reciprocal effects. However, some symbiotic relationships exhibit unilateral interactions, where only one species is affected while the other remains unaffected [1]. Two primary examples are commensalism, in which one species benefits without affecting the other, and amensalism, where one species is harmed while the other is unaffected [2].

Most mathematical studies of commensalism and amensalism have focused on two-species systems [3], [4], [5], [6], [7], [8], [9]. To the best of our knowledge, no previous study has investigated a three-species interaction model, in which one species simultaneously engages in both commensalism and amensalism. However, real ecosystems involve more complex interactions among three or more species. In this model, we consider the interaction between sea anemones, clownfish, and crustaceans that exhibit intertwined commensalism and amensalism. Sea anemone tentacles provide shelter for clownfish from predators while the sea anemone remains unaffected, thereby forming a commensalism [10]. Meanwhile, clownfish and crustaceans exhibit an amensalistic relationship, as clownfish are disadvantaged by the presence of crustaceans that compete for food resources [11]. Furthermore, an indirect biological interaction occurs between sea anemones and crustaceans coexisting in the same habitat. Sea anemones produce toxins that impair the

*Corresponding author. E-mail: wmuharini@ub.ac.id

Submitted: August 29, 2025 Reviewed: September 19, 2025 Accepted: October 21, 2025
DOI: https://doi.org/10.18860/cauchy.v10i2.36718

nervous system of nearby crustaceans, thereby reducing their survival rate [12]. Nevertheless, the movement of crustaceans around sea anemones facilitates greater food distribution to the anemones [13].

Motivated by the lack of studies on three-dimensional systems and the ecological interactions, we propose a three-species commensalism–amensalism model with Beddington–DeAngelis functional responses. The constructed model integrates the commensalism model with Beddington–DeAngelis functional responses by [9] and the linear amensalism model developed by [14]. Unlike previous models [9], [14], this formulation deliberately excludes external modifiers, such as delayed responses or external resource influences, to isolate and analyze the intrinsic effects of interspecies interactions. This study focuses on the fundamental mechanisms underlying both commensalism and amensalism by integrating their basic interaction structures into a unified three-species framework. This simplification allows a clearer examination of the combined dynamics of commensalism and amensalism, which have not been explicitly formulated in prior works. Moreover, this model incorporates biological interactions by sea anemones, clownfish, and crustaceans to enhance its ecological relevance. This paper aims to investigate the qualitative properties of solutions, determine the equilibrium points, and analyze the local stability properties of possible equilibrium points of the model. Finally, the numerical simulations are demonstrated to support the analytical findings.

2 Methods

1. First, we constructed this model based on the commensalism model developed by [9] and the amensalism model proposed by [14]. We constructed this model by considering ecologically realistic interactions inspired by sea anemones, clownfish, and crustaceans to enhance its ecological relevance.
2. Establish the positivity, boundedness, existence, and uniqueness of solutions to the system.
3. Next, we investigate the existence of equilibria and local stability properties of the equilibrium points of the model.
4. After that, to demonstrate the feasibility of our main results, we present numerical simulations using selected parameters.
5. Finally, we discuss the ecological significance of the obtained results and conclude the study by summarizing the main findings.

3 Results and Discussion

In this section, we analyse the proposed three-species commensalism–amensalism model and interpret its ecological implications. We begin by formulating the system of differential equations that describes the interactions among the neutral–commensalism, commensal–amensal, and neutral–amensalism species. We then establish basic analytical properties of the model, including positivity, boundedness, and well-posedness of solutions. After that, we characterise all biologically meaningful equilibria and study their local stability. Finally, we support the analytical results through numerical simulation and discuss the ecological meaning of the observed dynamical regimes.

3.1 Model Formulation

In the ecosystem, the neutral-commensalism species can be represented by sea anemones, which provide shelter for clownfish. In this relationship, the sea anemones neither benefits nor is harmed [10]. In addition to sea anemones and clownfish, there are crustaceans living in the same ecosystem. The movement of crustaceans can generate water currents that carry food particles,

which in turn increases the food availability for sea anemones when the crustaceans move nearby. Since sea anemones are sessile organisms attached to coral reefs or the seabed and unable to search for food actively [15], the presence of crustaceans indirectly enhances their food intake [13]. Therefore, this phenomenon increases the population growth rate of sea anemones. The quantity of additional food support provided by crustaceans is denoted by the parameter β. Therefore, the growth rate of the neutral–commensalism population is expressed as

$$\frac{dx}{dt} = x(a_1 - b_1 x) + \beta z. \tag{1}$$

The population of the commensal–amensal species grows with intrinsic growth rate a_2 and carrying capacity $\frac{a_2}{b_2}$. This species gains benefits from the neutral–commensalism species and suffers losses from the neutral–amensalism species, both of which affect its population dynamics. In the marine ecosystem, the commensal–amensal species is represented by the clownfish. Clownfish form a commensalism with sea anemones and an amensalism with crustaceans. The commensalism arises because clownfish gain shelter among the tentacles of sea anemones, while the anemones are unaffected.

The rate at which clownfish receive benefits from commensalism is denoted by c and depends on the population densities of both species. An increased clownfish population leads to intraspecific competition for limited space within anemones, reducing the benefit received per individual. Conversely, an increase in anemone density enhances the benefit only up to a certain limit, beyond which the effect saturates. This ecological behavior follows the Beddington–DeAngelis functional response $\frac{cx}{mx+ny+1}$, where m represents the saturation effect due to the increasing anemone population and n measures the intraspecific interference among clownfish.

In amensalism, clownfish and crustaceans compete for food resources. Because clownfish are confined to coral and anemone habitats, the presence of crustaceans significantly reduces their available food [11]. Meanwhile, crustaceans are not noticeably affected because they are capable of moving over long distances, unlike clownfish, which can only move around the anemone [16]. This creates an amensalism where the clownfish are harmed, but the crustaceans remain unaffected. The rate of loss experienced by the clownfish due to this amensalism is represented by α. Accordingly, the population dynamics of the commensal–amensal species are expressed as

$$\frac{dy}{dt} = y\left(a_2 - b_2 y + \frac{cx}{mx + ny + 1} - \alpha z\right). \tag{2}$$

The population of the neutral–amensalism species is assumed to grow logistically with intrinsic growth rate a_3 and carrying capacity $\frac{a_3}{b_3}$. In this ecosystem, the neutral–amensalism species is represented by crustaceans. As discussed earlier, crustaceans are not significantly affected by their interaction with clownfish. However, they can experience negative effects when moving close to sea anemones. Sea anemones possess toxic tentacles as a defense mechanism, and these toxins can impair the nervous system of nearby crustaceans, causing temporary paralysis. This paralysis reduces their mobility, productivity, and ability to evade predators [12]. Consequently, the growth rate of the crustacean population decreases with higher anemone density, which is represented by the inverse term $\frac{a_3}{x}$. Thus, the population dynamics of the neutral–amensal species are formulated as

$$\frac{dz}{dt} = z\left(\frac{a_3}{x} - b_3 z\right). \tag{3}$$

Based on the above explanations, a three-species commensalism–amensalism system that describes the population dynamics of neutral–commensalism, commensal–amensal, and neutral–amensalism species can be written as

$$\begin{aligned}\frac{dx}{dt} &= x(a_1 - b_1 x) + \beta z,\\ \frac{dy}{dt} &= y\left(a_2 - b_2 y + \frac{cx}{mx + ny + 1} - \alpha z\right),\\ \frac{dz}{dt} &= z\left(\frac{a_3}{x} - b_3 z\right),\end{aligned} \tag{4}$$

where $a_1, b_1, \beta, a_2, b_2, c, m, n, \alpha, a_3, b_3 > 0$.

3.2 Positivity and Boundedness of Solutions

This section establishes the positivity and the boundedness of solutions of the system 4. First, we show that the solutions remain positive for all $t \geq 0$. Second, we prove that the solutions are uniformly bounded, ensuring that the populations stay in a finite region.

Theorem 1. *All solutions of system (4) with initial values $x(0), y(0), z(0) > 0$ are positive for all $t \geq 0$. The solution $x(t)$ remains strictly positive for all $t \geq 0$.*

Proof: From model (4), we can solve $y(t)$ and $z(t)$ using initial condition $y(0), z(0) > 0$, the results are given by:

$$\begin{aligned}y(t) &= y(0) \exp \int_0^t \left(a_2 - b_2 y + \frac{cx}{mx + ny + 1} - \alpha z\right) dt,\\ z(t) &= z(0) \exp \int_0^t \left(\frac{a_3}{x} - b_3 z\right) dt.\end{aligned}$$

Hence, the solutions $y(t)$ and $z(t)$ remain positive for all $t \geq 0$ whenever $y(0), z(0) > 0$. To prove that $x(t)$ remains strictly positive, consider the first equation of system (4),

$$\frac{dx}{dt} = f(x, z) = x(a_1 - b_1 x) + \beta z.$$

On the boundary $x = 0$, and since $z(t)$ remains positive for all $t \geq 0$, we have

$$f(0, z) = \beta z \geq 0.$$

This implies that the vector field does not point outward from the nonnegative half-line. Hence, by the Nagumo tangency condition, the set $\{x \geq 0\}$ is forward invariant under the flow of (4).

Moreover, since $x(0) > 0$ and $f(0, z) = \beta z \geq 0$, the trajectory cannot touch or cross the boundary $x = 0$ in finite time. Indeed, if there exists $t^* > 0$ such that $x(t^*) = 0$, then from the first equation we have

$$\dot{x}(t^*) = \beta z(t^*) \geq 0.$$

Thus, at the boundary $x = 0$, the vector field does not point toward the region $x < 0$, and the solution cannot enter it.

Furthermore, because $z(t) > 0$ for all $t \geq 0$, it follows that $\dot{x}(t) = \beta z(t) > 0$ whenever $x(t) \to 0^+$. Therefore, $x(t)$ cannot reach 0 in finite time; instead, it is immediately pushed back into the region $x > 0$. Consequently,

$$x(t) > 0 \quad \text{for all } t \geq 0.$$

Theorem 2. *The solutions of system (4) are uniformly bounded.*

Proof: Define the function

$$N(t) = x(t) + y(t) + z(t),$$

Then, for every $\gamma > 0$, we get

$$\begin{aligned}\frac{dN(t)}{dt} + \gamma N &= (x(a_1 - b_1 x) + \beta z) + \left(a_2 y - b_2 y^2 + \frac{cxy}{mx + ny + 1} - \alpha zy\right) + \left(\frac{a_3 z}{x} - b_3 z^2\right) \\ &\quad + \gamma(x + y + z) \\ &\leq (\gamma + a_1)x - b_1 x^2 + \left(\gamma + a_2 + \frac{c}{m}\right) y - b_2 y^2 + (\gamma + \beta + a_3)\, z - b_3 z^2 \\ &\leq \frac{(\gamma + a_1)^2}{4b_1} + \frac{\left(\gamma + a_2 + \frac{c}{m}\right)^2}{4b_2} + \frac{(\gamma + \beta + a_3)^2}{4b_3} \\ &= K.\end{aligned}$$

Hence, we have

$$N(t) \leq \frac{K}{\gamma} + \left(N(0) - \frac{K}{\gamma}\right) e^{-\gamma t}$$

$$\lim_{t \to \infty} N(t) \leq \frac{K}{\gamma}.$$

Therefore, all solutions of system (4) are uniformly bounded by $\frac{K}{\gamma}$.

3.3 Existence and Uniqueness of Solutions

In this section, we show that the system (4) admits a unique solution within the region Ω. This follows from the Fundamental Existence–Uniqueness Theorem in [17], since the system satisfies the Lipschitz condition.

Theorem 3. *The system (4) admits a unique solution within the region*

$$\Omega := \left\{(x, y, z) \in \mathbb{R}^3_{\geq 0} : \max(|x|, |y|, |z|) \leq \tfrac{K}{\gamma}\right\}.$$

Proof: Let $\mathcal{X} = (x, y, z)$, $\bar{\mathcal{X}} = (\bar{x}, \bar{y}, \bar{z})$, and define

$$P(\mathcal{X}) = (P_1(\mathcal{X}), P_2(\mathcal{X}), P_3(\mathcal{X})),$$

where

$$P_1(\mathcal{X}) = \frac{dx}{dt}, \quad P_2(\mathcal{X}) = \frac{dy}{dt}, \quad P_3(\mathcal{X}) = \frac{dz}{dt}.$$

For any $\mathcal{X}, \bar{\mathcal{X}} \in \Omega$, it follows that

$$\begin{aligned}||P(\mathcal{X}) - P(\bar{\mathcal{X}})|| =& |P_1(\mathcal{X}) - P_1(\bar{\mathcal{X}})| + |P_2(\mathcal{X}) - P_2(\bar{\mathcal{X}})| + |P_3(\mathcal{X}) - P_3(\bar{\mathcal{X}})| \\ \leq& (a_1 + \tfrac{2Kb_1}{\gamma} + \tfrac{cK}{\gamma} + \tfrac{a_3\gamma}{K})|x - \bar{x}| + (a_2 + \tfrac{2Kb_2}{\gamma} + \tfrac{cK}{\gamma} + \tfrac{\alpha K}{\gamma})|y - \bar{y}| \\ &+ (\beta + \tfrac{\alpha K}{\gamma} + \tfrac{a_3\gamma}{K} + \tfrac{2Kb_3}{\gamma})|z - \bar{z}|.\end{aligned}$$

By setting

$$L = \max\left\{a_1 + \tfrac{2Kb_1}{\gamma} + \tfrac{cK}{\gamma} + \tfrac{a_3\gamma}{K},\ a_2 + \tfrac{2Kb_2}{\gamma} + \tfrac{cK}{\gamma} + \tfrac{\alpha K}{\gamma},\ \beta + \tfrac{\alpha K}{\gamma} + \tfrac{a_3\gamma}{K} + \tfrac{2Kb_3}{\gamma}\right\},$$

we obtain

$$||P(\mathcal{X}) - P(\bar{\mathcal{X}})|| \leq L||\mathcal{X} - \bar{\mathcal{X}}||.$$

Thus, $P(\mathcal{X})$ satisfies the Lipschitz condition in Ω.

3.4 Equilibrium Points

In this section, we show all possible equilibrium points of the system (4).

Theorem 4. *The system (4) has four equilibrium points, which* $E_1\left(\frac{a_1}{b_1},0,0\right)$, $E_2\left(\frac{a_1}{b_1},y_2,0\right)$, *and* $E_3(x_3,0,z_3)$ *always exist. The other equilibrium point* $E_4(x^*,y^*,z^*)$ *exist if* $B_3<0$, *where* $B_3=\frac{1}{b_2 n}\left(\frac{\alpha a_3}{b_3 x^*}(mx^*+1)-a_2(mx^*+1)-cx^*\right)$ *and* x^* *is the unique positive real root of cubic equation* $x^3-\frac{a_1}{b_1}x^2-\frac{a_3\beta}{b_1 b_3}=0$.

Proof: The equilibrium points of the system (4) are identified by setting the following equations

$$\begin{aligned} x(a_1-b_1x)+\beta z&=0\\ y\left(a_2-b_2y+\frac{cx}{mx+ny+1}-\alpha z\right)&=0\\ z\left(\frac{a_3}{x}-b_3z\right)&=0. \end{aligned} \tag{5}$$

First, we can verify that $E_1\left(\frac{a_1}{b_1},0,0\right)$ always exist.

Second, when $E_2\left(\frac{a_1}{b_1},y_2,0\right)$, we determine that y_2 is all feasible positive real solutions of the following quadratic equation:

$$A_1y^2+A_2y+A_3=0, \tag{6}$$

where

$$A_1=1,\quad A_2=\frac{a_1m}{b_1n}+\frac{1}{n}-\frac{a_2}{b_2},\quad \text{and}\quad A_3=-\left(\frac{a_1a_2m}{b_1b_2n}+\frac{a_2}{b_2n}+\frac{a_1c}{b_1b_2n}\right).$$

The discriminant of equation (6) is $\Delta=(A_2)^2-4A_3$. We can solve that $\Delta>0$ because $(A_2)^2>0$ and $-4A_3>0$. It guarantees that (6) have two distinct real roots, i.e. y_{2_1} and y_{2_2}. Moreover, we can solve the multiplication of y_{2_1} and y_{2_2} as $y_{2_1}y_{2_2}=\frac{A_3}{A_1}<0$. The negative result implies that the roots have opposite signs. Hence, equation (6) has a unique positive real root given by $y_2=\frac{-A_2+\sqrt{(A_2)^2-4A_3}}{2}$. Therefore, $E_2\left(\frac{a_1}{b_1},y_2,0\right)$ where $y_2=\frac{-A_2+\sqrt{(A_2)^2-4A_3}}{2}$ always exist.

Next, by setting $y=0$, we get $E_3(x_3,0,z_3)$, where $z_3=\frac{a_3}{b_3x_3}$ and x_3 is all real positive roots of the following cubic equation:

$$x^3-\frac{a_1}{b_1}x^2-\frac{a_3\beta}{b_1b_3}=0. \tag{7}$$

By the transformation $x=u-\frac{a_1}{3b_1}$, equation (7) reduces to the depressed cubic

$$u^3+3pu+q=0, \tag{8}$$

with $p=-\frac{{a_1}^2}{9{b_1}^2}$ and $q=-\left(\frac{a_3\beta}{b_1b_3}+\frac{2{a_1}^3}{27{b_1}^3}\right)$. By applying Lemma 3.1 in [18], the depressed cubic equation (8) admits exactly one real positive root explicitly. Furthermore, we can observe that equation (7) has only one change of sign. By using *Descartes' rule of sign* in [19], it is verified that the equation (7) has one positive root. Thus, x_3 is a unique real positive root and satisfies $z_3=\frac{a_3}{b_3x_3}$, so the equilibrium point $E_3(x_3,0,z_3)$ always exist.

Lastly, we determine the coexistence equilibrium point $E_4(x^*,y^*,z^*)$. From equation (5), by arranging $z^*=\frac{a_3}{b_3x^*}$ and substituting to $\frac{dx}{dt}=0$, we have a cubic equation similar with (7). Hence, there is a unique real positive root x^* and $x^*=x_3$, that also satisfies $z_3=z^*=\frac{a_3}{b_3x^*}$. Furthermore, by substituting x^*,z^* to $\frac{dy}{dt}=0$, we get y^* is all possible positive real solutions of the following quadratic equation:

$$B_1y^2+B_2y+B_3=0, \tag{9}$$

where

$$B_1 = 1,\ B_2 = \frac{mx^* + 1}{n} + \frac{1}{b_2}\left(\frac{\alpha a_3}{b_3 x^*} - a_2\right),\ B_3 = \frac{1}{b_2 n}\left(\frac{\alpha a_3}{b_3 x^*}(mx^* + 1) - a_2(mx^* + 1) - cx^*\right).$$

Since the discriminant $\Delta = B_2^2 - 4B_3 > 0$, the quadratic equation admits two distinct real roots. Because the product of the roots is B_3 and their sum is $-B_2$, then there are three possible cases for the existence of positive real roots of (9). We can verify as follows:

1. If $B_2 < 0$ and $B_3 > 0$, both roots would be positive. Let $mx^* + 1 = S$, then

$$B_2 = \frac{S}{n} + \frac{1}{b_2}\left(\frac{\alpha a_3}{b_3 x^*} - a_2\right) \tag{10}$$

and

$$B_3 = \frac{1}{b_2 n}\left(S\left(\frac{\alpha a_3}{b_3 x^*} - a_2\right) - cx^*\right). \tag{11}$$

From (10), we get

$$\frac{\alpha a_3}{b_3 x^*} - a_2 = b_2 B_2 - \frac{b_2 S}{n}. \tag{12}$$

Then, B_3 reduced to

$$B_3 = \frac{SB_2}{n} - \frac{S^2}{n^2} - \frac{cx^*}{nb_2}. \tag{13}$$

By letting $B_2 < 0$, necessarily implies that $B_3 < 0$, with the result that the case where $B_2 < 0$ and $B_3 > 0$ cannot occur.

2. If $B_2 > 0$ and $B_3 < 0$, equation (9) has exactly one positive root. We can verify from equation (13) by letting $B_3 < 0$, we get $B_2 < \frac{S}{n} + \frac{cx^*}{b_2 S}$. Let $\frac{S}{n} + \frac{cx^*}{b_2 S} = B_2^*$, then the case where $B_2 > 0$ and $B_3 < 0$ exist if $0 < B_2 < B_2^*$.
3. If $B_2 < 0$ and $B_3 < 0$, equation (9) again has exactly one positive root. This case exists and is proven in case 1, because letting $B_2 < 0$, necessarily implies that $B_3 < 0$.

Hence, equation (9) has a real positive root given by

$$y^* = \frac{-B_2 + \sqrt{B_2^2 - 4B_3}}{2}.$$

Therefore, the coexistence equilibrium point $E_4(x^*, y^*, z^*)$ exists where $z^* = \frac{a_3}{b_3 x^*}$, $x^* = x_3$ is a unique real positive root of (7) and

$$y^* = \frac{-B_2 + \sqrt{B_2^2 - 4B_3}}{2}, \tag{14}$$

if $B_3 < 0$ holds.

3.5 Local Stability Analysis

In this section, we obtain the local stability of the equilibrium points of the system (4) by evaluating the Jacobian matrix of (4). The Jacobian matrix of the system (4) is given by

$$\begin{bmatrix} a_1 - 2b_1 x^* & 0 & \beta \\ P & Q & -\alpha y^* \\ -\frac{{a_3}^2}{b_3 (x^*)^3} & 0 & -\frac{a_3}{x^*}, \end{bmatrix} \tag{15}$$

where $Q = a_2 - 2b_2 y^* + \frac{cx^*}{mx^* + ny^* + 1} - \frac{cnx^* y^*}{(mx^* + ny^* + 1)^2} - \frac{\alpha a_3}{b_3 x^*}$, $P = \frac{cy^*}{mx^* + ny^* + 1} - \frac{cmx^* y^*}{(mx^* + ny^* + 1)^2}$, and (x^*, y^*, z^*) is the equilibrium points of (4).

Theorem 5. *The equilibrium points E_1 and E_2 are unstable.*

Proof: The Jacobian matrix (15) evaluated at E_1 and E_2 are, respectively, $J(E_1) = \begin{bmatrix} -a_1 & 0 & \beta \\ 0 & a_2 + \frac{a_1 c}{m a_1 + b_1} & 0 \\ 0 & 0 & \frac{a_3 b_1}{a_1} \end{bmatrix}$, and

$$J(E_2) = \begin{bmatrix} -a_1 & 0 & \beta \\ \frac{cy_2}{mx_2+ny_2+1} - \frac{cmx_2y_2}{(mx_2+ny_2+1)^2} & a_2 - 2b_2y_2 + \frac{cx_2}{mx_2+ny_2+1} - \frac{cnx_2y_2}{(mx_2+ny_2+1)^2} & -\alpha y_2 \\ 0 & 0 & \frac{a_3 b_1}{a_1} \end{bmatrix}.$$

The eigenvalues of $J(E_1)$ are $\lambda_1 = -a_1, \lambda_2 = a_2 + \frac{a_1 c}{m a_1 + b_1}, \lambda_3 = \frac{a_3 b_1}{a_1}$. Also, the eigenvalues of $J(E_2)$ are $\lambda_1 = -a_1, \lambda_2 = a_2 - 2b_2y_2 + \frac{cx_2}{mx_2+ny_2+1} - \frac{cnx_2y_2}{(mx_2+ny_2+1)^2}, \lambda_3 = \frac{a_3 b_1}{a_1}$. Each of the matrices $J(E_1)$ and $J(E_2)$ have at least one positive eigenvalue. Hence, the equilibrium points E_1 and E_2 are unstable.

Theorem 6. *The neutral-only equilibrium point E_3 is locally asymptotically stable when $c < c^*$, $\frac{\alpha a_3}{b_3 x_3} > a_2$, and $\frac{\beta}{b_3 x_3} > 1$, where $c^* = \left(\frac{1}{x_3}\right)\left(\frac{\alpha a_3}{b_3 x_3} - a_2\right)(mx_3 + 1)$.*

Proof: The Jacobian matrix (15) at E_3 is

$$J(E_3) = \begin{bmatrix} a_1 - 2b_1x_3 & 0 & \beta \\ 0 & a_2 + \frac{cx_3}{mx_3+1} - \frac{\alpha a_3}{b_3 x_3} & 0 \\ -\frac{{a_3}^2}{b_3 {x_3}^3} & 0 & -\frac{a_3}{x_3} \end{bmatrix}. \tag{16}$$

The characteristics equation of $J(E_3)$ is

$$\left(a_2 + \frac{cx_3}{mx_3+1} - \frac{\alpha a_3}{b_3 x_3} - \lambda\right)\left(d_0\lambda^2 + d_1\lambda + d_2\right) = 0, \tag{17}$$

where $d_0 = 1$, $d_1 = 2b_1x_3 + \frac{a_3}{x_3} - a_1$ and $d_2 = 2a_3b_1 + \frac{{a_3}^2\beta}{b_3 {x_3}^3} - \frac{a_1 a_3}{x_3}$. The roots of (17) have negative real parts if $a_2 + \frac{cx_3}{mx_3+1} - \frac{\alpha a_3}{b_3 x_3} < 0$. Thus, we have $c < c^*$, where $c^* = \left(\frac{1}{x_3}\right)\left(\frac{\alpha a_3}{b_3 x_3} - a_2\right)(mx_3 + 1)$ and $\frac{\alpha a_3}{b_3 x_3} > a_2$. Based on the Routh-Hurwitz criterion, the real parts of the roots of the quadratic part of (17) are negative if

$$d_0 = 1 > 0, \quad |d_1| > 0, \quad \text{and} \quad \begin{vmatrix} d_1 & 1 \\ 0 & d_2 \end{vmatrix} = d_1 d_2 > 0 \tag{18}$$

Since $d_1 > 0$, then $d_2 > 0$. We can solve that

$$d_1 = 2b_1x_3 + \frac{a_3}{x_3} - a_1 > 0 \quad \Rightarrow \quad 2b_1x_3 + \frac{a_3}{x_3} > a_1 \tag{19}$$

and

$$d_2 = 2a_3b_1 + \frac{{a_3}^2\beta}{b_3 (x_3)^3} - \frac{a_1 a_3}{x_3} > 0 \quad \Rightarrow \quad 2b_1x_3 + \frac{a_3\beta}{b_3 {x_3}^2} > a_1. \tag{20}$$

By eliminating (20) by (19), we can solve that $0 < \frac{a_3}{x_3}\left(\frac{\beta}{b_3 x_3} - 1\right)$. Therefore, λ_2, λ_3 in (17) is negative if $\frac{\beta}{b_3 x_3} > 1$. Since $c < c^*$, $\frac{\alpha a_3}{b_3 x_3} > a_2$, and $\frac{\beta}{b_3 x_3} > 1$, then the E_3 is locally asymptotically stable.

Theorem 7. *The coexistence equilibrium point E_4 is locally asymptotically stable when $c < c^{**}$, $2b_2y^* + \frac{\alpha a_3}{b_3 x^*} > a_2$, and $\frac{\beta}{b_3 x^*} > 1$, where $c^{**} = \left(\frac{1}{x^*}\right)\left(2b_2y^* + \frac{\alpha a_3}{b_3 x^*} - a_2\right)\left(\frac{(mx^*+ny^*+1)^2}{mx^*+1}\right)$.*

The characteristic equation of matrix (15) at $E_4(x^*, y^*, z^*)$ is given by

$$(Q - \lambda)\left(e_0\lambda^2 + e_1\lambda + e_2\right) = 0, \tag{21}$$

where $e_0 = 1$, $e_1 = 2b_1x^* + \frac{a_3}{x^*} - a_1$ and $e_2 = 2a_3b_1 + \frac{{a_3}^2\beta}{b_3(x^*)^3} - \frac{a_1a_3}{x^*}$. The roots of equation (21) have negative real parts if $Q < 0$. Thus, we have $c < c^{**}$, where

$$c^{**} = \left(\frac{1}{x^*}\right)\left(2b_2y^* + \frac{\alpha a_3}{b_3x^*} - a_2\right)\left(\frac{(mx^* + ny^* + 1)^2}{mx^* + 1}\right)$$

and

$$2b_2y^* + \frac{\alpha a_3}{b_3x^*} > a_2.$$

Next, with the Routh-Hurwitz criterion, the roots of the quadratic part of (21) have negative real parts if

$$e_0 = 1 > 0, \quad |e_1| > 0, \quad \text{and} \quad \begin{vmatrix} e_1 & 1 \\ 0 & e_2 \end{vmatrix} = e_1e_2 > 0 \tag{22}$$

It has been mentioned before that $x_3 = x^*$, then we have $e_0 = d_0$, $e_1 = d_1$, and $e_2 = d_2$. Hence, we can get the same criterion for λ_2, λ_3 in E_4 stability as in E_3, that is negative if $\frac{\beta}{b_3x_3} = \frac{\beta}{b_3x^*} > 1$. Hence, the E_4 is locally asymptotically stable if $c < c^{**}$, $2b_2y^* + \frac{\alpha a_3}{b_3x^*} > a_2$, and $\frac{\beta}{b_3x^*} > 1$.

We summarize the stability condition of each equilibrium point through the Table 1.

Table 1: Stability condition of the equilibrium points of model (4)

Equilibria	Type of Stability	Stability Condition
$E_1(\frac{a_1}{b_1}, 0, 0)$	Unstable	-
$E_2\left(\frac{a_1}{b_1}, y_2, 0\right)$	Unstable	-
$E_3(x_3, 0, z_3)$	Asymptotically stable	$c < \left(\frac{1}{x_3}\right)\left(\frac{\alpha a_3}{b_3x_3} - a_2\right)(mx_3 + 1)$, $\frac{\alpha a_3}{b_3x_3} > a_2$, $\frac{\beta}{b_3x_3} > 1$
$E_4(x^*, y^*, z^*)$	Asymptotically stable	$c < \left(\frac{1}{x^*}\right)\left(2b_2y^* + \frac{\alpha a_3}{b_3x^*} - a_2\right)\left(\frac{(mx^*+ny^*+1)^2}{mx^*+1}\right)$, $2b_2y^* + \frac{\alpha a_3}{b_3x^*} > a_2$, $\frac{\beta}{b_3x^*} > 1$

3.6 Numerical Simulation

In this section, we present numerical simulations using the 4th-order Runge-Kutta to demonstrate the feasibility of our main results. To prevent the risk of division by zero in the term $\frac{a_3}{x}$, a small positive threshold was introduced by setting $x = 10^{-6}$ whenever $x = 0$. This approach is commonly used to maintain numerical stability and avoid computational errors without significantly affecting the system's dynamics. For all simulations, hypothetical parameter values were employed, as empirical data were unavailable. These values satisfy the necessary conditions established through the stability analysis. All parameter sets used in this numerical simulation are shown in Table 2.

Firstly, we conducted a simulation under the necessary condition for the stability of E_3 using the parameter set 1 in Table 2. From Table 2, using parameter set 1, we obtain $c < c^*$, $\frac{\beta}{b_3x_3} > 1$, and $\frac{\alpha a_3}{b_3x_3} > a_2$, which satisfies the necessary condition for E_3 stability. The numerical simulation of the solution and phase portrait captures the behavior of E_3. As shown in Fig. 1, x increases rapidly at the beginning and then settles at a constant value at $x \approx 13.361$. Similarly, z increases slightly and stabilizes at $z \approx 0.748446$. Meanwhile, y decreases drastically and converges to $y = 0$. The results confirm the locally asymptotically stable behavior of E_3. Furthermore, the phase portrait in Fig. 2 llustrates that the solution of system (4) asymptotically approaches the equilibrium point $E_3 = (13.361, 0, 0.748446)$.

Table 2: Parameter sets for numerical simulation

No.	Parameter Set	Equilibrium Points	Values of Required Condition
1	$a_1 = 0.25, b_1 = 0.025,$ $\beta = 1.5, a_2 = 0.4,$ $b_2 = 0.04, a_3 = 1,$ $b_3 = 0.1, m = 0.3,$ $n = 0.5, \alpha = 0.7, c = 0.03$	E_3 $x_3 \approx 13.361$ $y_3 = 0$ $z \approx 0.748446$	$c < c^* = 0.04644770517$ $\frac{\beta}{b_3 x_3} = 1.1227 > 1$ $\frac{\alpha a_3}{b_3 x_3} = 0.5239 > a_2$
2	$a_1 = 0.25, b_1 = 0.025,$ $\beta = 1.5, a_2 = 0.4,$ $b_2 = 0.04, a_3 = 1,$ $b_3 = 0.1, m = 0.3,$ $n = 0.5, \alpha = 0.7, c = 0.2$	E_4 $x^* = 13.361$ $y^* = 5.50835$ $z^* = 0.748446$	$c < c^{**} = 0.5083893560$ $\frac{\beta}{b_3 x^*} = 1.1227 > 1$ $B_3 = -102.5808 < 0$ $B_2 = 13.1144 > 0$ $2b_2 y^* + \frac{\alpha a_3}{b_3 x^*} = 2.7396 > a_2$
3	$a_1 = 0.25, b_1 = 0.025,$ $\beta = 1.5, a_2 = 0.8,$ $b_2 = 0.04, a_3 = 1,$ $b_3 = 0.1, m = 0.3,$ $n = 0.9, \alpha = 0.3, c = 1.7$	E_4 $x^* = 13.361$ $y^* = 31.4378$ $z^* = 0.748446$	$c < c^{**} = 32.14562241$ $\frac{\beta}{b_3 x^*} = 1.1227 > 1$ $B_3 = -710.9960 < 0$ $B_2 = -8.8219 < 0$ $2b_2 y^* + \frac{\alpha a_3}{b_3 x^*} = 0.9646 > a_2$

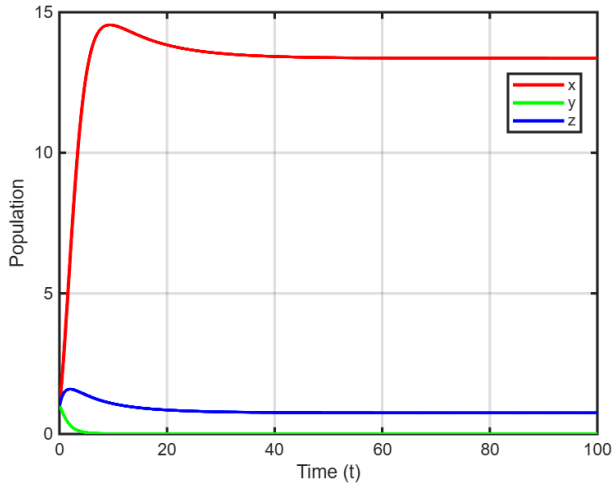

Figure 1: Solution of x, y and z for the stability of E_3

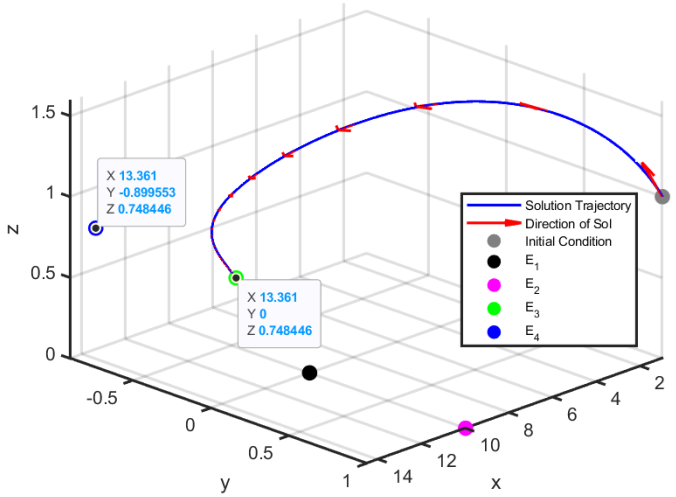

Figure 2: Phase portrait illustration of E_3

Next, we conducted a simulation under the necessary condition of E_4 stability. We first consider the condition where $B_2 > 0$ and $B_3 < 0$ holds, using parameter set 2 at Table 2. In Table 2 and parameter set 2, we obtain $c < c^{**}$, $\frac{\beta}{b_3 x^*} > 1$, and $2b_2 y^* + \frac{\alpha a_3}{b_3 x^*} > a_2$, which fulfills the necessary condition for the local stability of E_4. According to Fig. 3, the curves of x and z show a trend similar to that in Fig. 1. Meanwhile, y decreases slightly at first and then grows until it stabilizes at $y \approx 5.50835$. The phase portrait in Fig. 4 validates that the solution tend and stabilize to $E_4 = (13.361, 5.50835, 0.748446)$ asymptotically.

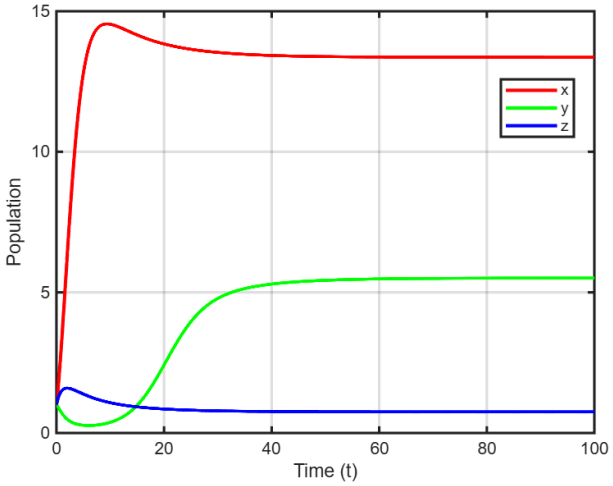

Figure 3: Solution of x, y and z for the stability of E_4, where $B_2 > 0$ and $B_3 < 0$

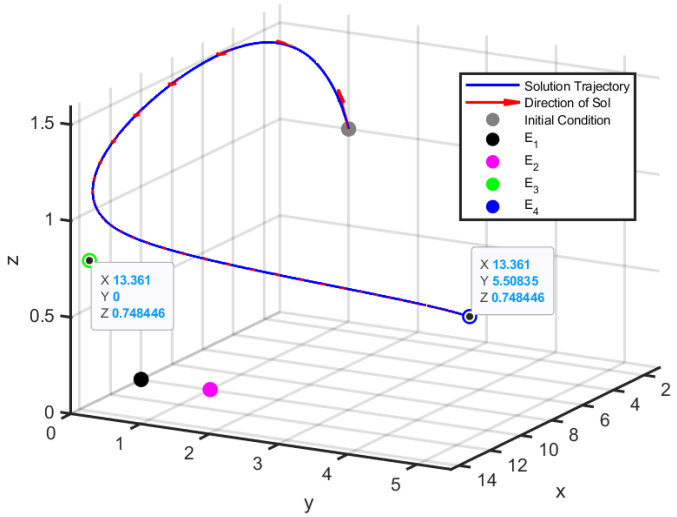

Figure 4: Phase portrait illustration of E_4 where $B_2 > 0$ and $B_3 < 0$

Finally, we consider the condition of E_4 where $B_2 < 0$ and $B_3 < 0$ with parameter set 3 at Table 2. In Table 2 and parameter set 2, where $B_2 < 0$ and $B_3 < 0$, we obtained $c < c^{**}$, $\frac{\beta}{b_3 x^*} > 1$, and $2b_2 y^* + \frac{\alpha a_3}{b_3 x^*} > a_2$. These results confirm the consistency of the previous stability analysis and satisfy the conditions required for the local stability of E_4. As shown in Fig. 5, the curves of x and z show similar trends to those observed when $B_2 > 0$. The trend of their curves is similar to that observed in Fig. 1. However, the y curve increases rapidly from the beginning until it stabilizes at $y \approx 31.4378$. Moreover, phase portrait Fig. 6 demonstrate that the solutions are locally asymptotically stable at the equilibrium point.

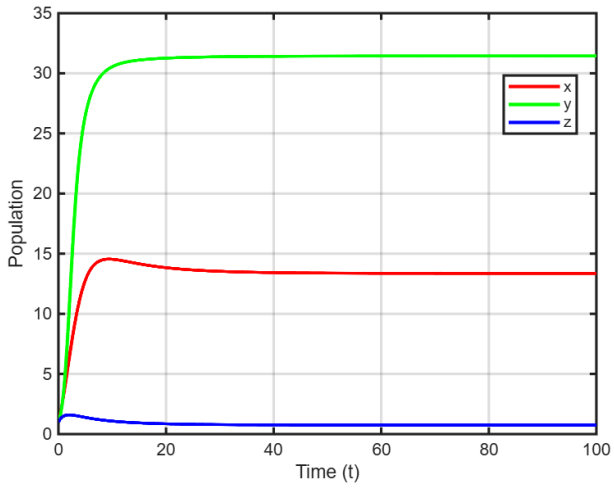

Figure 5: Solution of x, y and z for the stability of E_4, where $B_2 < 0$ and $B_3 < 0$

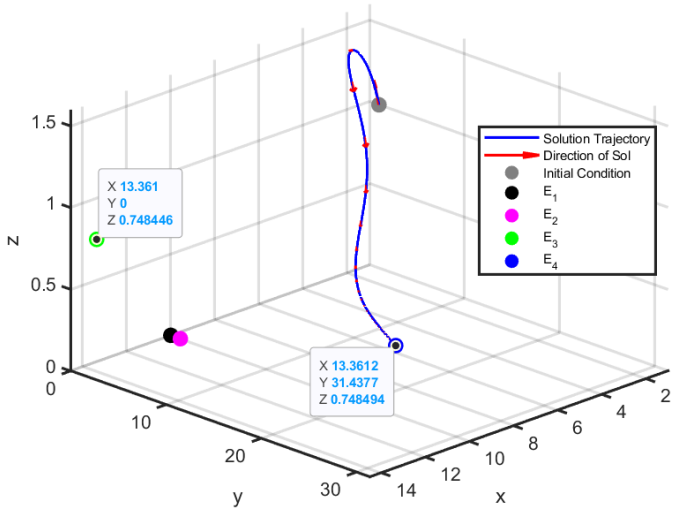

Figure 6: Phase portrait illustration of E_4 where $B_2 > 0$ and $B_3 < 0$

3.7 Discussion

This study demonstrates the influence of neutral species in supporting the abundance of commensal-amensal species. From the local stability analysis of E_2, it is shown that when one neutral species does not coexist with the commensal-amensal species and the other neutral species, the system becomes unstable. However, if the commensal-amensal species coexist with all neutral species, the dynamics of their population growth become stable. This finding is supported by the stability analysis of E_4, confirmed by the simulation results and phase portrait illustrations in Fig. 3, Fig. 5, Fig. 4, and Fig. 6. On the other hand, all neutral species can survive and maintain stable populations independently, even when the commensal–amensal populations go extinct. This is revealed by the stability of E_3 and illustrated in Fig. 1 and Fig. 2. These results suggest that, in real ecosystems, neutral species can persist without relying on commensal-amensal species.

In line with this study, the two species commensalism model reveals that the commensal population grows stably when coexisting with neutral species. While the neutral species can possess stable dynamics without the commensal species [20]. A similar outcome is observed in the two species amensalism model, where the system can be stable when amensal coexist with neutral species, while the neutral species itself can admit stability [14]. Hence, the neutral species has an important role in maintaining the ecosystem dynamics.

Moreover, from the stability analysis and numerical simulations, we observe that the stability

of each equilibrium point depends on the value of c, the rate at which clownfish receive benefits from commensalism. Moreover, it has been mentioned in the existence of equilibrium point analysis, that $x_3 = x^*$, which means $\frac{\alpha a_3}{b_3 x_3} = \frac{\alpha a_3}{b_3 x^*} > a_2$ and support stability condition of $E_3(x^*, 0, z^*)$. This result shows that, if the rate of loss due to amensalism is weighted by the carrying capacity of the neutral amensalism and larger than the intrinsic growth of the commensal-amensal, then the commensal-amensal species goes extinct. However, in the stability of E_4, where the system is stable in the presence of all species, we have the condition $2b_2 y^* + \frac{\alpha a_3}{b_3 x^*} > a_2$. This implies that the population density of the commensal–amensal species plays a significant role in sustaining their presence in the ecosystem.

Furthermore, because many factors influence the dynamics of the ecosystem in terms of three species commensalism-amensalism, future research could explore more complex interaction structures, such as incorporating environmental fluctuations, time delays, or stochastic effects. In addition, extending the model into higher-dimensional ecological networks may provide deeper insights into how neutral species contribute to the overall stability and resilience of ecosystems.

4 Conclusion

The three species commensalism-amensalism model with Beddington-DeAngelis functional response describes the complexity of the ecosystem's dynamics among more than two species, in which one species simultaneously engages in both commensalistic and amensalistic interactions. This model involves neutral-commensalism species, commensal–amensal species, and neutral-amensalism species. In the real ecosystem, this model reflects the interaction among sea anemones, clownfish, and crustaceans. We examine the positivity, boundedness, existence, and uniqueness of the solution, and identify four equilibrium points. The first two equilibria are always unstable. Moreover, the system admits a stability condition when the equilibrium point denotes the existence of only neutral species and the coexistence of commensal-amensal with neutral species.

From an ecological perspective, the stability of the three-species system is ensured only when all neutral species coexist. If any neutral species is absent, the system becomes unstable. In contrast, stability can still be maintained even in the absence of the commensal–amensal species. This finding underlines the critical role of neutral species in sustaining community persistence. Nevertheless, the existence of commensal-amensal species can be enhanced by their own population density. More broadly, this model extends classical two-species frameworks to a more ecologically relevant three-species setting, offering insight into how unilateral symbioses shape ecosystem stability.

CRediT Authorship Contribution Statement

Nada Shofiyya: Conceptualization, Model Formulation, Methodology, Formal Analysis, Visualization, Writing–Original Draft. **Wuryansari Muharini Kusumawinahyu:** Supervision, Model Formulation-Review, Formal Analysis-Review, Writing–Review, Visualization-Review. **Ummu Habibah:** Supervision, Model Formulation-Review, Writing–Review, Visualization-Review.

Declaration of Generative AI and AI-assisted technologies

Generative AI tools (ChatGPT, OpenAI) were used only for language editing (grammar, spelling, and clarity) and minor support in idea formulation. All scientific content and conclusions are the sole responsibility of the authors.

Declaration of Competing Interest

The authors declare no competing interests.

Funding and Acknowledgments

This research received no external funding.

Data and Code Availability

The data and code supporting the findings of this study are available from the corresponding author upon reasonable request and subject to confidentiality agreements.

References

[1] A. Mougi, "The roles of amensalistic and commensalistic interactions in large ecological network stability," *Scientific Reports*, vol. 6, no. 1, p. 29 929, 2016. DOI: 10.1038/srep29929.

[2] J. Veiga, "Commensalism, amensalism, and synnecrosis," in *Encyclopedia of Evolutionary Biology*, R. M. Kliman, Ed., Oxford: Academic Press, 2016, pp. 322–328. DOI: 10.1016/B978-0-12-800049-6.00189-X.

[3] Y. Chong and F. Chen, "Global stability, bifurcations and chaos control in a discrete amensalism model with cover and saturation effect," *Journal of Applied Analysis and Computation*, vol. 15, no. 5, pp. 2977–3003, 2025.

[4] K. Fang, Y. Wang, F. Chen, and X. Chen, "Dynamics of a modified lotka–volterra commensalism system incorporating allee effect and symmetric non-selective harvest," *Symmetry*, vol. 17, no. 6, 2025. DOI: 10.3390/sym17060852.

[5] A. Ditta, P. A. Naik, R. Ahmed, et al., "Exploring periodic behavior and dynamical analysis in a harvested discrete-time commensalism system," *International Journal of Dynamics and Control*, vol. 13, p. 63, 2025. DOI: 10.1007/s40435-024-01551-z.

[6] D. Luo and Q. Wang, "Global dynamics of a beddington–deangelis amensalism system with weak allee effect on the first species," *Applied Mathematics and Computation*, vol. 408, p. 126 368, 2021. DOI: 10.1016/j.amc.2021.126368.

[7] X. Guan and F. Chen, "Dynamical analysis of a two species amensalism model with beddington–deangelis functional response and allee effect on the second species," *Nonlinear Analysis: Real World Applications*, vol. 48, pp. 71–93, 2019. DOI: 10.1016/j.nonrwa.2019.01.002.

[8] M. Zhao and Y. Du, "Stability and bifurcation analysis of an amensalism system with allee effect," *Advances in Difference Equations*, vol. 2020, no. 1, p. 341, 2020. DOI: 10.1186/s13662-020-02804-9.

[9] M. Qu, "Dynamical analysis of a beddington–deangelis commensalism system with two time delays," *Journal of Applied Mathematics and Computing*, vol. 69, no. 6, pp. 4111–4134, 2023. DOI: 10.1007/s12190-023-01913-4.

[10] E. F. Camp, J.-P. A. Hobbs, M. De Brauwer, A. J. Dumbrell, and D. J. Smith, "Cohabitation promotes high diversity of clownfishes in the coral triangle," *Proceedings of the Royal Society B: Biological Sciences*, vol. 283, no. 1827, p. 20 160 277, 2016. DOI: 10.1098/rspb.2016.0277.

[11] C. Alwi, W. Muzammil, and S. Susiana, "Makanan dan kebiasaan makan kepiting merah (thalamita spinimana, dana 1852) di perairan dompak, tanjungpinang, kepulauan riau," *Journal of Marine Research*, vol. 11, no. 4, pp. 729–737, 2022. DOI: 10.14710/jmr.v11i4.34488.

[12] L. Cariello et al., "Calitoxin, a neurotoxic peptide from the sea anemone calliactis parasitica: Amino-acid sequence and electrophysiological properties," *Biochemistry*, vol. 28, no. 6, pp. 2484–2489, 1989, PMID: 2567180. DOI: 10.1021/bi00432a020.

[13] J. Fish and S. Fish, *A Student's Guide to the Seashore*. Cambridge University Press, 2011. Available online.

[14] M. Zhao, Y. Ma, and Y. Du, "Global dynamics of an amensalism system with michaelis-menten type harvesting," *Electronic Research Archive*, vol. 31, no. 2, pp. 549–574, 2023. DOI: 10.3934/era.2023027.

[15] J. L. Clarke, P. A. Davey, and N. Aldred, "Sea anemones (exaiptasia pallida) use a secreted adhesive and complex pedal disc morphology for surface attachment," *BMC Zoology*, vol. 5, no. 1, p. 5, 2020. DOI: 10.1186/s40850-020-00054-6.

[16] K. R. N. Florko et al., "Tracking movements of decapod crustaceans: A review of a half-century of telemetry-based studies," *Marine Ecology Progress Series*, vol. 679, pp. 219–239, 2021. DOI: 10.3354/meps13904.

[17] L. Perko, *Differential Equations and Dynamical Systems* (Texts in Applied Mathematics), 3rd ed. New York, NY: Springer Science+Business Media, 2001, vol. 7. DOI: 10.1007/978-1-4613-0003-8.

[18] Y. Cai, C. Zhao, W. Wang, and J. Wang, "Dynamics of a leslie–gower predator–prey model with additive allee effect," *Applied Mathematical Modelling*, vol. 39, no. 7, pp. 2092–2106, 2015. DOI: 10.1016/j.apm.2014.09.038.

[19] J. D. Murray, *Mathematical Biology: I. An Introduction* (Interdisciplinary Applied Mathematics), 3rd. New York, Berlin, Heidelberg: Springer, 2002, vol. 17. DOI: 10.1007/b98868.

[20] F. Chen, Z. Li, and L. Chen, "Dynamic behaviors of a stage structure commensalism system with holling type ii commensalistic benefits," *WSEAS Transactions on Mathematics*, vol. 21, pp. 810–824, 2022. DOI: 10.37394/23206.2022.21.93.